JOURNAL OF MATERIALS SCIENCE 30 (1995) 4609–4616

# Ductile and strong aluminium–matrix titanium aluminide composite formed *in situ* from aluminium, titanium dioxide and sodium hexafluoroaluminate

YUYONG CHEN, D. D. L. CHUNG
*Composite Materials Research Laboratory, State University of New York at Buffalo, Buffalo, NY 14260–4400, USA*

An aluminium–matrix $TiAl_3$-particle (1–2 μm) composite exhibiting high tensile ductility (22%), high tensile strength (235 MPa) and a grain size of 50 μm was made by a new *in situ* method involving reactions between Al, $TiO_2$ and $Na_3AlF_6$, which were subjected to stir casting at 900 °C. The strength and ductility were higher than those of an aluminium–matrix $TiAl_3$-particle $Al_2O_3$-particle composite made *in situ* by reacting Al with $TiO_2$ (without $Na_3AlF_6$). This is due to the ability of $Na_3AlF_6$ to enhance the reduction of $TiO_2$ and $Al_2O_3$, thus resulting in more $TiAl_3$ and a smaller grain size.

## 1. Introduction

Materials that are both strong and ductile are the dream of engineers. Unfortunately, the reality is that a strong material tends to be not very ductile, while a ductile material tends to be not very strong. For example, aluminium metal is rather weak but ductile, while aluminium–matrix composites commonly containing SiC particles or whiskers as the reinforcement is strong but rather brittle. Aluminium alloys that are relatively strong, e.g. Al–Cu, Al–Si and Al–Zn, also tend to be relatively brittle. In this work, we have developed an aluminium–matrix composite (or dispersion-strengthened metal) which is both ductile and strong; the tensile strength is even higher than those of aluminium–matrix composites containing SiC whiskers or particles, while the tensile ductility is almost as high as that of pure aluminium. This new composite (or alloy) contained about 5 vol % titanium aluminide ($TiAl_3$) particles of size about 1–2 μm and was formed *in situ* from aluminium, titanium dioxide ($TiO_2$) particles and sodium hexafluoroaluminate ($Na_3AlF_6$). The *in situ* formation caused the reinforcement ($TiAl_3$) to be fine and well bonded to the aluminium matrix.

The *in situ* formation of composites is a subject of considerable recent research [1]. A commonly used reaction for the *in situ* formation is

$$5Al(\text{liquid}) + 3MO(\text{solid}) \rightarrow Al_2O_3(\text{solid}) + 3Al\text{–}M(\text{liquid})$$

where $MO$ is a certain metal oxide. This reaction results in an Al–$M$ matrix composite containing $Al_2O_3$ particles as the reinforcement [2]. In particular, this reaction had been conducted for the case of the metal oxide being $TiO_2$ [3]. In this case, the reaction takes the form

$$7Al(\text{liquid}) + 3TiO_2(\text{solid}) \rightarrow 2Al_2O_3(\text{solid}) + 3Al\text{–}Ti(\text{liquid})$$

A second reaction scheme, which is less commonly used, is

$$2Al + 3MO \rightarrow Al_2O_3 + 3M$$

$$M + Al \rightarrow MAl$$

where $MAl$ is a metal aluminide. This sequence of reactions results in an aluminium–matrix composite containing $Al_2O_3$ particles as well as $MAl$ particles. It has been carried out for the case of the metal oxide being $TiO_2$ [4] ; in this case, the sequence of reactions is

$$4Al + 3TiO_2 \rightarrow 2Al_2O_3 + 3Ti$$

$$Ti + Al \rightarrow TiAl$$

and

$$Ti + 3Al \rightarrow TiAl_3$$

and results in two kinds of titanium aluminides, i.e. TiAl and $TiAl_3$.

In this work, a third reaction scheme was used for the first time for *in situ* composite formation. This scheme involves the sequence

$$2TiO_2 + 2Na_3AlF_6 \rightarrow 2Na_2TiF_6 + Na_2O + Al_2O_3$$

$$2Na_2TiF_6 + 6Al \rightarrow 4NaF + 4F_2 + 2TiAl_3$$

$$Al_2O_3 + 2Na_3AlF_6 \rightarrow 3NaO + 4Al + 6F_2$$

and results in an aluminium–matrix composite containing $TiAl_3$ particles as the reinforcement. The

0022–2461 

reactant $Na_3AlF_6$ is a flux that is commonly used in foundry work for reducing metal oxides. Due to the ability of $Na_3AlF_6$ to reduce $TiO_2$ as well as $Al_2O_3$, $TiO_2$ was consumed fully in the reaction and no $Al_2O_3$ remained in the resulting composite.

Although *in situ* composites are the subject of numerous papers, the papers are focused on the processing methods and provide rather little data, if any, on the tensile properties of the resulting composites. In this work, the tensile properties of the authors' new *in situ* composite were measured, thereby revealing the unusual combination of high ductility and high strength exhibited by the composite.

For the sake of comparison, this paper reports on the comparison of the composite made from $TiO_2$ and $Na_3AlF_6$ using the third reaction scheme with that made from $TiO_2$ using a combination of the other two reaction schemes. The former composite exhibited higher tensile strength, modulus and ductility than the latter composite, thus indicating the virtue of the third reaction scheme.

## 2. Experimental procedure

### 2.1. Materials

The aluminium used was commercial 6061 aluminium alloy. The $TiO_2$ particles of size 40 μm were obtained from Johnson Matthey Co. The $Na_3AlF_6$ particles of size 40 μm were obtained from J. T. Baker, Inc.

### 2.2. Composite fabrication

Two *in situ* composite fabrication methods were used, corresponding to a combination of the first and second reaction schemes and to the third scheme mentioned in the Introduction, and labelled method A and method B, respectively.

In method A, $TiO_2$ particles were heated in air at 300 °C for 4 h and then added to the surface of the liquid aluminium at 900 °C. The amount of $TiO_2$ was 20% of the weight of the aluminium. After this, the slurry was stirred intermittantly at 900 °C for a period of about 30 min in order to allow the reactions to occur. About 20% of the $TiO_2$ powder was not reacted and remained on the surface of the liquid aluminium; it was removed before casting.

In method B, $TiO_2$ particles were mixed with $Na_3AlF_6$ particles in the weight ratio 1:1 and then heated at 300 °C for 4 h. The mixture was then slowly added to the surface of the liquid aluminium at 900 °C. The amount of the mixture was 40% of the weight of the aluminium. After this, the slurry was stirred intermittantly at 900 °C for a period of about 30 min in order to allow the reactions to occur. All of the $TiO_2$ was reacted, so that no $TiO_2$ particle remained on the surface of the liquid aluminium.

In both methods A and B, immediately after stirring the slurry and subsequently allowing the slurry to sit for 5–10 min, the slurry was poured into a cylindrical steel mould of diameter 30 mm and height 40 mm at room temperature. After casting and subsequent solidification at a cooling rate of about 200 °C $min^{-1}$

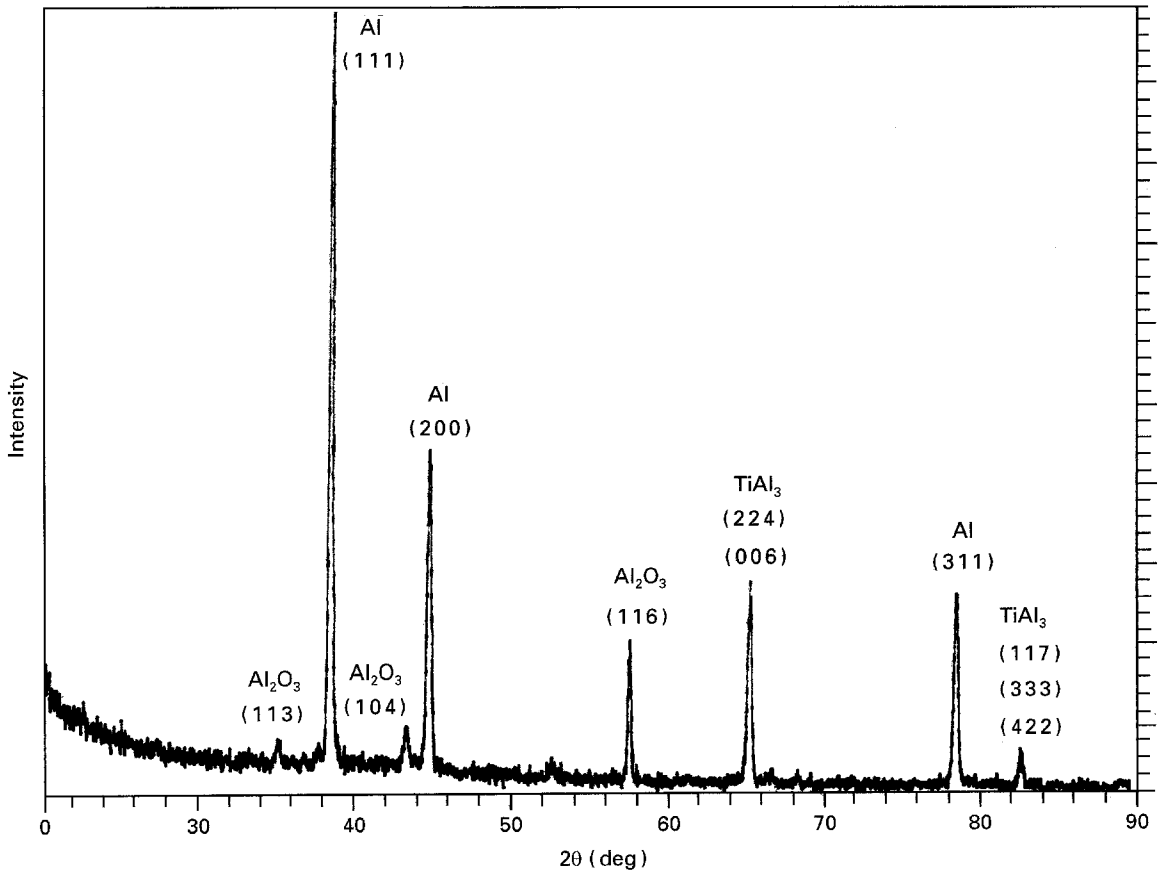


*Figure 1* X-ray diffraction pattern of composite A, i.e. composite made by method A. Each peak is labelled by the phase and its Miller indices.

(unless stated otherwise), the composite was heated at 519 °C for 1 h, then quenched into water at room temperature, and then heated at 165 °C for 18 h, in accordance with the $T_6$ heat treatment procedure for the 6061 aluminium alloy.

For the sake of comparison, the 6061 alloy by itself was subjected to the same casting and heat treatment procedure, and its properties were compared to those of the composites.

## 2.3. Composite characterization

X-ray diffraction (using Cu$K_\alpha$ radiation) of the composites obtained by methods A and B showed that the composite obtained by method A consisted of aluminium, $TiAl_3$ and $\alpha$-$Al_2O_3$ (Fig. 1), whereas that obtained by method B consisted of aluminium and $TiAl_3$ (Fig. 2). No phase other than these was observed. To help observe the phases other than Al, most of the Al in both composites had been etched away (in a solution with 20% HCl, 20% $H_2SO_4$ and 60% $H_2O$) at room temperature for 30 min prior to diffraction. Furthermore, to help the collection of the composite particles (after etching) for diffraction, the particle sizes of the phases other than Al were made larger by using a lower cooling rate of 10 °C min$^{-1}$. When the ordinary cooling rate of 200 °C min$^{-1}$ was used, the phases other than Al could not be observed by X-ray diffraction.

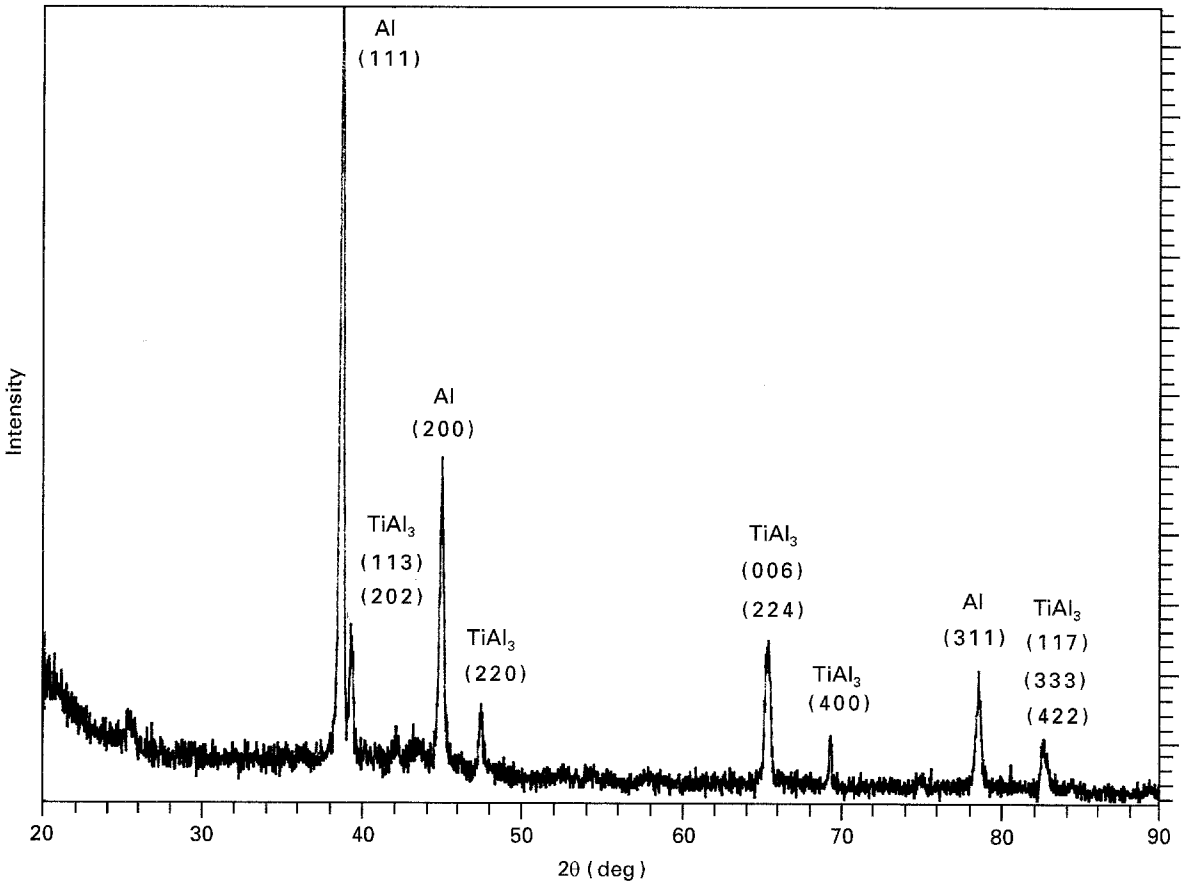


*Figure 2* X-ray diffraction pattern of composite B, i.e. composite made by method B. Each peak is labelled by the phase and its Miller indices.

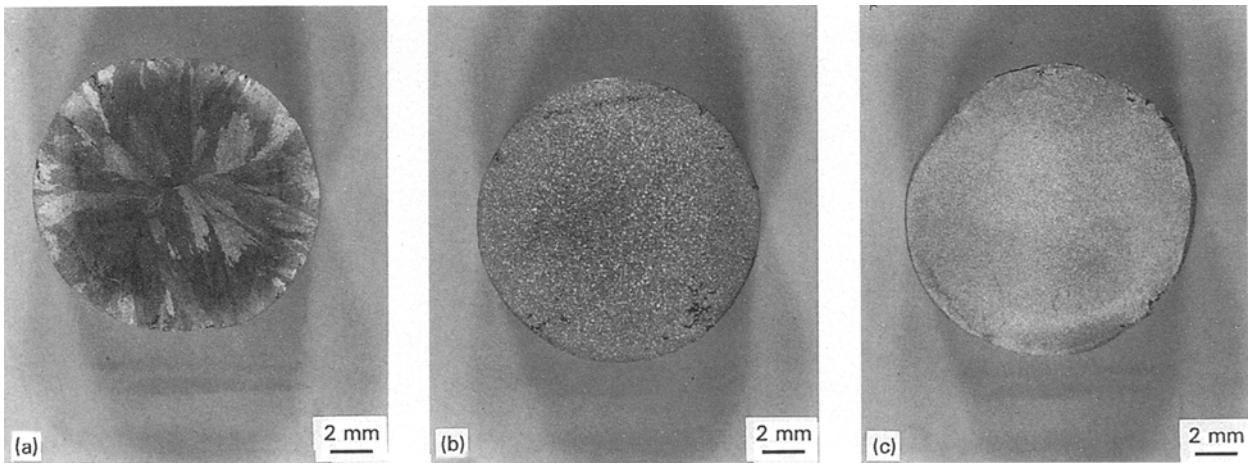


*Figure 3* Optical micrographs of (a) the aluminium matrix, (b) composite A, and (c) composite B. All samples were etched in 10% NaOH solution at about 70 °C for 3 min.

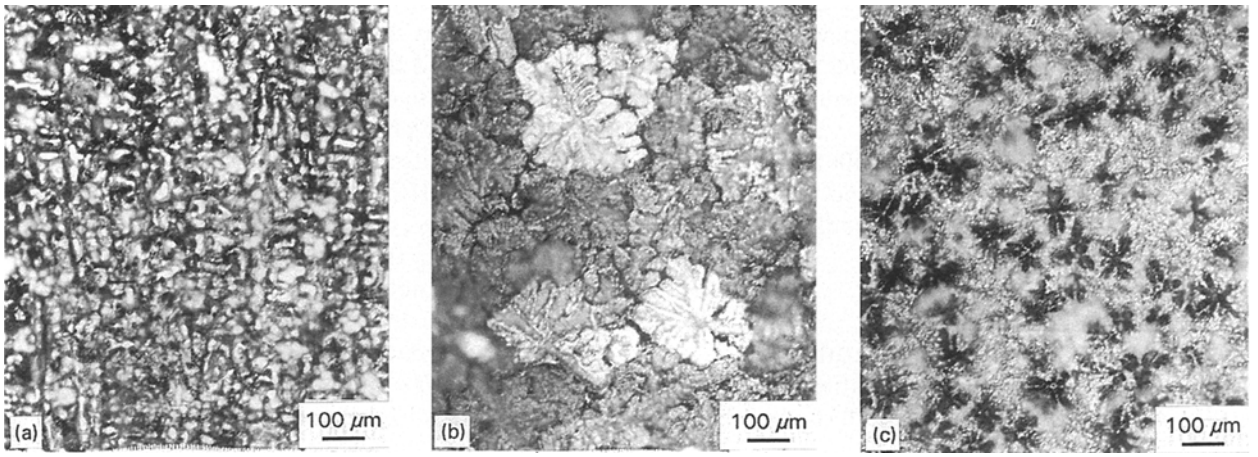


*Figure 4* Optical micrographs of (a) the aluminium matrix, (b) composite A, and (c) composite B. The magnification is higher than that of Fig. 3. All samples were lightly etched in Keller's agent (15 vol % $HNO_3$, 10 vol % HCl, 5 vol % HF and 70 vol % $H_2O$).

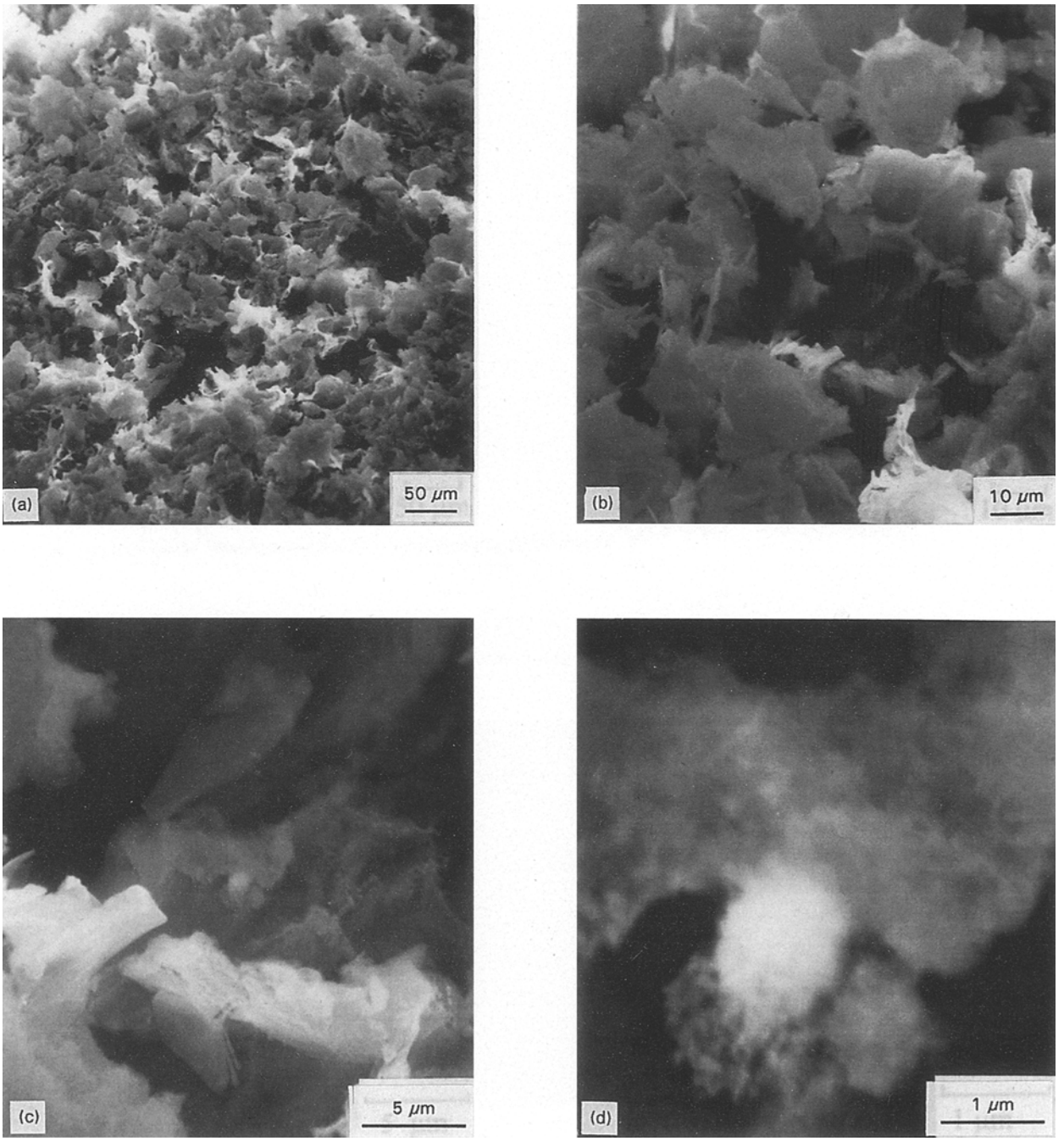


*Figure 5* SEM photographs at various magnifications of composite B after heavy etching in 20% NaOH solution.

Optical microscopic examination was conducted of the polished and lightly etched sections of

1. the aluminium by itself,
2. the composite made by method A, and
3. the composite made by method B.

The aluminium by itself exhibited columnar grains of size $2 \times 15$ mm (Fig. 3a) and columnar dendrites within the grains (Fig. 4a), while the composites exhibited much finer microstructure (Fig. 3b,c and 4b,c). The microstructure of the composite made by method B (Fig. 3c) was even finer than that of the composite made by method A (Fig. 3b). Both composites were uniform in microstructure. The Al grains were equiaxed and of 0.2 and 0.05 mm size for the composites made by methods A (Fig. 4b) and B (Fig. 4c), respectively. The dendrites were equiaxed in both composites. The $TiAl_3$ particles were

TABLE I Microhardness and hardness. The standard deviations (based on six data points for each type of specimen) are shown in parentheses

| Material | Microhardness (HV) | Hardness (BHN) |
|---|---|---|
| Al matrix | 51.2( $\pm$ 0.6) | 38.1( $\pm$ 2.1) |
| Composite A | 57.5( $\pm$ 0.7) | 44.9( $\pm$ 2.6) |
| Composite B | 62.7( $\pm$ 0.7) | 64.8( $\pm$ 2.3) |

TABLE II Tensile properties. The standard deviations (based on three data points for each type of specimen) are shown in parentheses

| Material | Strength (MPa) | Ductility (%) |
|---|---|---|
| Al matrix | 164( $\pm$ 3.0) | 18.7( $\pm$ 1.2) |
| Composite A | 214( $\pm$ 1.5) | 17.3( $\pm$ 1.3) |
| Composite B | 235( $\pm$ 2.0) | 22.0( $\pm$ 1.0) |

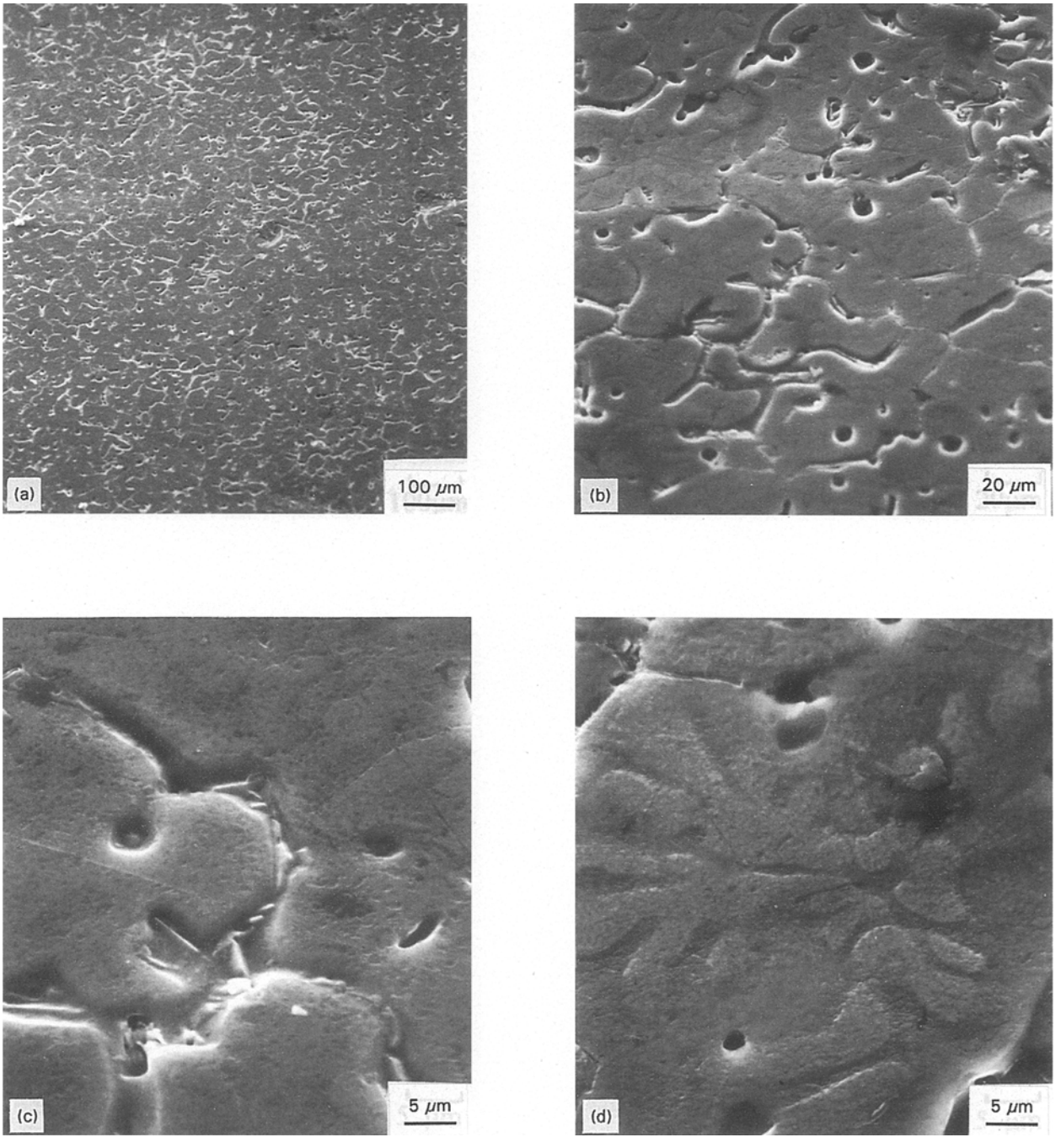


*Figure 6* SEM photographs at various magnifications of composite A after light etching.

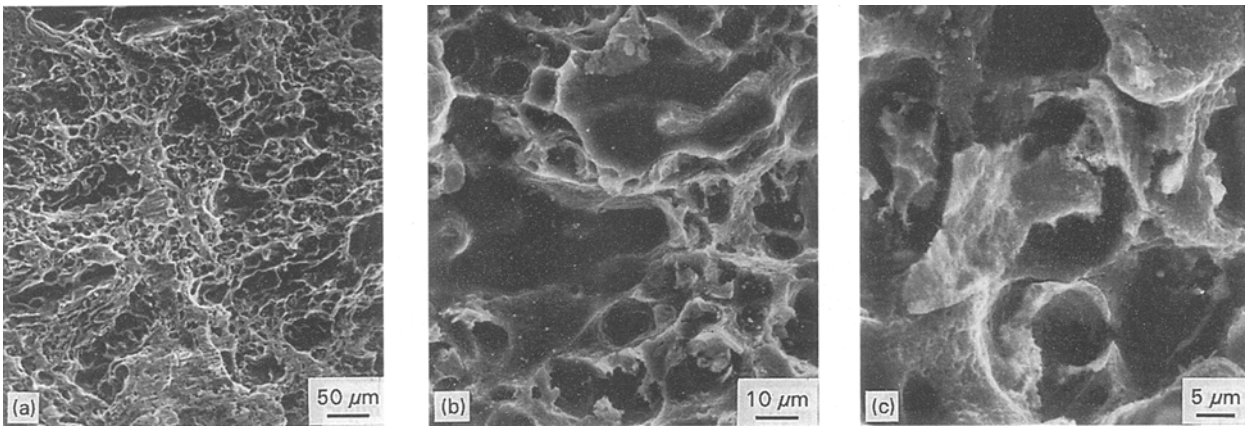


*Figure 7* SEM photographs at various magnifications of the tensile fracture surface of the aluminium matrix.

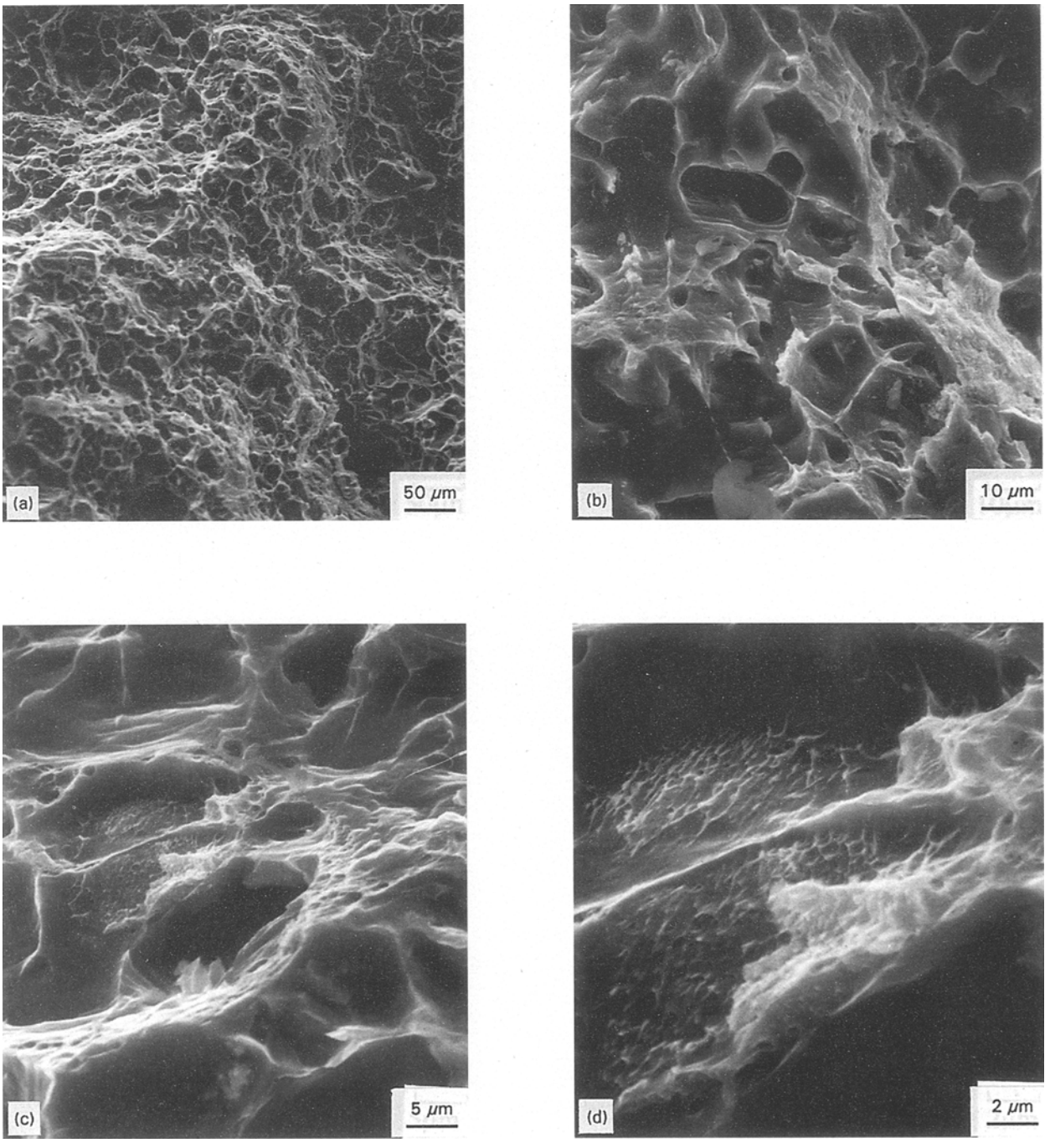


*Figure 8* SEM photographs at various magnifications of the tensile fracture surface of composite B.

of 1–2 μm size in the composites made by methods A and B, as shown by scanning electron microscopy (SEM) for the composite made by method B (after heavy etching in 20% NaOH solution) in Fig. 5d (which is a high magnification view of the centre of Fig. 5c), in which the bright region is relatively rich in Ti (as shown by X-ray spectroscopy). The $TiAl_3$ particles were not visible at lower magnifications (Fig. 5a, b). The volume fraction of $TiAl_3$ was estimated to be 5% in the composite made by method B, but was significantly lower in the composite made by method A, due to the fact that not all of the added $TiO_2$ was reacted in method A. The grain boundaries were relatively rich in Si and Mg (originating from the 6061 Al alloy matrix); the grain boundaries are shown by SEM in Fig. 6 for the composite made by method A (after light etching). The dendrites within a grain are shown in Fig. 6d for the composite made by method A.

Table I gives the microhardness (Vicker's) and hardness (Brinell) of the aluminium by itself and of the composites made by methods A and B. The composite made by method B (abbreviated composite B) was considerably harder (in both scales) than that made by method A (abbreviated composite A). Both composites were harder than the aluminium by itself.

Table II gives the tensile properties, which were obtained on dog-bone shaped specimens using a Sintech two-dimensional screw-type mechanical testing system. The ductility was obtained by measuring the change in distance between two lines drawn perpendicular to the stress axis. The tensile strength and ductility were higher in composite B than composite A. Both composites exhibited higher strength than the Al matrix. The ductility of composite B was even higher than that of the matrix alloy, because of its much finer microstructure. Figs 7 and 8 show the fracture surfaces (viewed by SEM) of the Al matrix and composite B, respectively. Indeed Fig. 8 shows a larger proportion of dimples on the fracture surface than Fig. 7. In addition, Fig. 8d (a high magnification view of the left central part of Fig. 8c) shows a relatively Ti rich region (as shown by X-ray spectroscopy) inside a hole in the fracture surface.

Table III gives the coefficient of thermal expansion (CTE), which was obtained by using a Perkin–Elmer model 7 dynamic mechanical analyser operated at a heating rate of 5 °C $min^{-1}$. The CTE was similar for composites A and B. Both composites exhibited lower CTE than the matrix alloy.

## 3. Discussion

The new composite (alloy) provided by this work is composite B. (It is debatable whether this material should be classified as a composite or an alloy.) Its tensile properties (without secondary processing for mechanical property enhancement) are compared to those of other aluminium–matrix composites and aluminium alloys in Table IV. Comparison shows that composite B is outstandingly high in ductility compared to other composites and alloys, and is higher in

TABLE III Coefficient of thermal expansion ($10^{-6}$ °$C^{-1}$) for various temperature ranges. The standard deviations (based on three specimens of each type) are shown in parentheses

| Material | 30–100 °C | 30–200 °C | 30–300 °C |
|---|---|---|---|
| Al matrix | 23.12( ± 0.01) | 23.35( ± 0.07) | 24.05( ± 0.03) |
| Composite A | 19.40( ± 0.31) | 19.72( ± 0.23) | 20.49( ± 0.07) |
| Composite B | 19.29( ± 0.21) | 19.80( ± 0.30) | 20.46( ± 0.14) |

TABLE IV Comparison of the tensile properties of the aluminium–matrix composites of this work and those of previous work, together with selected aluminium alloys

| Material | Ductility (%) | Strength (MPa) | Reference |
|---|---|---|---|
| Composite B | 22 | 235 | This work |
| Composite A | 17.3 | 214 | This work |
| [a]Al/12 vol % SiCw | 6.9 | 181 | [5] |
| [a]Al/10 Mg/10 vol %SiCw | 5.4 | 227 | [5] |
| [b]Al/10 vol % SiCp | 24 | 145 | [6] |
| [b]Al/10 vol % SiCw | 14 | 191 | [6] |
| [b]Al/20 vol % SiCp | 10 | 200 | [6] |
| [c]A356/10 vol % SiCp | 4.5 | 223 | [7] |
| [c]F3s/10 vol % SiCp | 1.57 | 221.4 | [8] |
| [c]F3A/10 vol % SiCp | 1.30 | 228.2 | [8] |
| [c]LM25/5 vol % graphite | 2.3 | 136 | [9] |
| [d]2024/20 wt% $Al_2O_3$ | 0.3 | 207 | [10] |
| 3033H14(Al–1.2 Mn) | 17 | 159 | [11] |
| 5052H34(Al–2.5 Mg–0.25 Cr) | 4 | 262 | [11] |
| 2024T6(Al–4.4 Cu–1.5 Mg–0.6 Mn) | 5 | 442 | [11] |
| 6061T6(Al–1.0 Mg–0.6 Si–0.27 Cu–0.2 Cr) | 10 | 290 | [11] |
| 7075T6(Al–5.6 Zn–2.5 Mg–1.6 Cu–0.23 Cr) | 8 | 504 | [11] |
| 413.0(Al–12 Si–2Fe) | 2.5 | 297 | [11] |
| 356.0(Al–7Si–0.3 Mg), $T_6$ | 3 | 229 | [11] |

[a] Made by liquid metal infiltration.
[b] Made by powder metallurgy and rolling.
[c] Made by casting.
[d] Made by compocasting.

strength than all composites listed and some alloys. Thus, both high ductility (very high) and high strength (moderately high) are exhibited by composite B. These properties of composite B are attributed to the fine microstructure (small Al grain size and small $TiAl_3$ particle size) and the good bonding between $TiAl_3$ and the Al matrix, as made possible by the *in situ* composite formation. Composite B was higher in strength and ductility than composite A because of composite B's smaller grain size and higher $TiAl_3$ volume fraction; the smaller grain size was a consequence of the higher $TiAl_3$ volume fraction. The *in situ* formation involved stir casting and made use of inexpensive equipment and raw materials. Moreover, the process can be easily scaled up. Thus, composite B is also attractive economically. It is expected to be valuable for a large variety of structural and industrial applications.

## 4. Conclusions

A new *in situ* composite fabrication method was used to produce an aluminium–matrix composite containing about 5 vol % $TiAl_3$ particles of 1–2 μm size. The composite exhibited high tensile strength and high ductility. The method involved stir casting in air a slurry consisting of molten aluminium, $TiO_2$ particles and $Na_3AlF_6$ particles. Reactions among these ingredients resulted in $TiAl_3$. The composite had a grain size of 50 μm. It exhibited higher tensile strength, ductility, microhardness and hardness than an *in situ* aluminium–matrix $Al_2O_3$-particle $TiAl_3$-particle composite made by stir casting a slurry consisting of molten aluminium and $TiO_2$ particles. This is due to the ability of $Na_3AlF_6$ to enhance the reduction of $TiO_2$ and $Al_2O_3$, thus resulting in more $TiAl_3$. The ductility of the new composite was much higher and its strength was higher than those of *ex situ* aluminium–matrix SiC whisker (up to 12 vol %) or particle (up to 20 vol %) composites.


## Acknowledgements

This work was supported by the Advanced Research Projects Agency of the US Department of Defense and the Center for Electronic and Electro-Optic Materials of the State University of New York at Buffalo.


## References


1. M. J. KOCZAK and M. K. PREMKUMAR, JOM **45** (1993) 44.
2. MAKOTO KOBASHI and TAKAO CHOH, Paper presented at the Third International SAMPE Metals Conference Covina, CA, October 1992, p. M600–M610.
3. P. C. MAITY, S. C. PANIGRAHI and P. N. CHAKRABORTY, *Scripta Metall.* **28** (1993) 549.
4. D. Z. WANG, Z. R. LIU, C. K. YAO and M. YAO, *J. Mater. Sci. Lett.* **12** (1993) 1420.
5. YUYONG CHEN and D. D. L. CHUNG, to be published.
6. V. V. BHANUPRASAD, *Int. J. Powder Metallurgy* **27** (1991) 227.
7. H. RIBERS, *Mater. Sci. Technol.* **6** (1990) 621.
8. A. LABIB, *Mater. Sci. Eng.* **A160** (1993) 81.
9. U. T. S. PILLAI, *ibid.* **A169** (1993) 93.
10. F. M. HOSKING, *J. Mater. Sci.* **17** (1982) 477.
11. W. F. SMITH, "Foundations of materials science and engineering", 2nd Edn. (McGraw-Hill, New York, 1993), p. 475.



*Received 27 June 1994*
*and accepted 15 March 1995*